Metastable states influence on the magnetic behavior of the triangular lattice: Application to the spin-chain compound $Ca_3Co_2O_6$

R. Soto,[1] G. Martínez,[1,2] M. N. Baibich,[2] J. M. Florez,[1] and P. Vargas[1,3,*]
[1] *Departamento de Física, Universidad Técnica Federico Santa María, P.O. Box 110-V, Valparaíso, Chile*
[2] *Instituto de Física, Universidade Federal do Rio Grande do Sul, 91501-970 Porto Alegre-RS, Brasil*
[3] *Max-Planck Institute for Solid State Research, Heisenbergstrasse 1, D-70569, Stuttgart, Germany*
(Dated: November 28, 2008)

It is known that the spin-chain compound $Ca_3Co_2O_6$ exhibits very interesting plateaus in the magnetization as a function of the magnetic field at low temperatures. The origin of them is still controversial. In this paper we study the thermal behavior of this compound with a single-flip Monte Carlo simulation on a triangular lattice and demonstrate the decisive influence of metastable states in the splitting of the ferrimagnetic 1/3 plateau below 10 K. We consider the $[Co_2O_6]_n$ chains as giant magnetic moments described by large Ising spins on planar clusters with open boundary conditions. With this simple frozen-moment model we obtain stepped magnetization curves which agree quite well with the experimental results for different sweeping rates. We describe particularly the out-of-equilibrium states that split the low-temperature 1/3 plateau into three steps. They relax thermally to the 1/3 plateau, which has long-range order at the equilibrium. Such states are further analyzed with snapshots unveiling a domain-wall structure that is responsible for the observed behavior of the 1/3 plateau. A comparison is also given of the exact results in small triangular clusters with our Monte Carlo results, providing further support for our thermal description of this compound.

PACS numbers: 75.25.+z, 75.30.Kz, 75.40.Mg, 75.60.-d

I. INTRODUCTION

Low-dimensional interacting spins always reveal very interesting magnetic properties, as well as new electronic transport phenomena [1, 2, 3, 4]. Along this line, systems with geometric frustration have long attracted our attention because the ground-state properties, like degeneracy, are usually responsible for peculiar behaviors at low temperatures. Included are exotic magnetization dependences with external fields in hysteresis curves, for example. One group of compounds that exhibits such properties is the family $CsCoX_3$, where X stands for Cl or Br [5]. These materials are unidimensional Ising-like magnetic systems. The spin chains are arranged on a triangular lattice, while the intra- and interchain exchange couplings are both antiferromagnetic.

Another fascinating spin-chain family of compounds with triangular arrangements has the formula A'_3ABO_6 (where A' may be Ca or Sr, whereas A and B are transition metals). One particular system that caught our attention is $Ca_3Co_2O_6$ [6, 7, 8, 9, 10, 11, 12, 13, 14, 15, 16, 17, 18, 19, 20, 21, 22, 23, 24], which has a rombohedral structure composed of large chains of $[Co_2O_6]_n$ along the c-axis of a corresponding hexagonal lattice. The Ca atoms are located among those chains. The chains are made of alternating face-sharing CoO_6 trigonal prisms and CoO_6 octahedra. Each Co chain is thus surrounded by six equally spaced Co chains forming an hexagonal lattice in the ab-plane (see Figure 1).

Generally, the long Co-Co interchain distance (5.3 Å), in $Ca_3Co_2O_6$, compared to the short Co-Co intrachain distance (2.6 Å), ensures the hierarchy of the magnetic exchange energies, $J_{\text{intra}} \gg J_{\text{inter}}$, in modulus. This fact, together with a strong spin-orbit coupling [25, 26], provide a high uniaxial anisotropy along the c-axis. Neutron diffraction studies [7], among others, have revealed a ferromagnetic intrachain interaction ($J_{\text{intra}} < 0$), while an antiferromagnetic interchain interaction ($J_{\text{inter}} > 0$) was observed in the ab-plane. Consequently, it is very plausible to describe the magnetism of this compound by considering an Ising triangular lattice of large magnetic frozen-moments linked to the chains, each one playing the role of a giant spin, pointing either up or down.

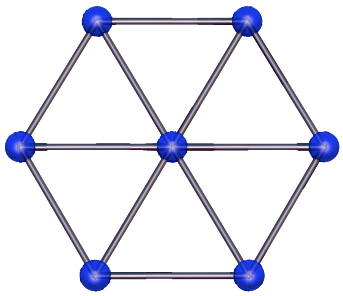

FIG. 1: Hexagonal lattice of Co chains projected onto the ab-plane (blue points) of the spin-chain compound $Ca_3Co_2O_6$. Each chain is ordered ferromagnetically and is coupled antiferromagnetically to its neighbors.

*Electronic address: vargas.patricio@gmail.com

One of the interesting features observed in $Ca_3Co_2O_6$ is the appearance of plateaus in the magnetization curve M vs H, below $T_C = 25$ K, when the magnetic field is applied along the chains (c-axis). For temperatures in the range, $10\,\mathrm{K} \leq T \leq T_C$, it is observed a rapidly increase of M with H. Close to zero field, the magnetization reaches a plateau at the value of $M_s/3$ (M_s, the saturation magnetization is $\sim 4.8\,\mu_\mathrm{B}$/f.u.). This value remains constant up to $H_c \approx 3.6$ T, where the magnetization springs up to its saturation value M_s. Otherwise, when $T \leq 10$ K, called the ferrimagnetic region, the observed plateau at $M_s/3$, splits into three small steps, changing at fields $H = 1.2$ T, 2.4 T, 3.6 T, respectively. Much effort has been done to understand such behavior, and it is still a controversial matter. Some papers [16, 21, 24] roused the question that this behavior might be related to experiments involving single-molecule magnets (SMM) [27, 28], where a Quantum Tunneling of the Magnetization (QTM) is realized [29]. We restrain such statement, at least for temperatures above 4K, as we demonstrate here and leave the question of QTM effects to be searched below 2K, according to the experimental situation.

We follow instead the line of reasoning that metastable states, or peculiar mozaic configurations, might play a role in the splitting of the magnetization of this frustrated material, as first suggested by Maignan *et al.* [9]. Therefore, we started a simulation along the lines given by Kudasov [30], who predicted an opening of the 1/3 plateau using Monte Carlo analysis at $T = 0$. More recently, Yao *et al.* [31, 32], studied this compound with numerical Monte Carlo simulations on finite clusters. The latter works describe the system with an Ising Hamiltonian on a triangular lattice, using periodic boundary conditions. Despite their results reproduce the steps width, $\Delta H \sim 1.2$ T, in the magnetization curves, they do not find a clear-cut (*equilibrium*) configuration that explains the splitting of the 1/3 plateau. In this work we report on a similar study using the same model, but considering instead free boundary conditions on an anisotropic system, which is added for completion with the intrinsic dipolar term at the end. We apply non-equilibrium techniques on this system. We detect in this form, by sweeping the field at different rates, the presence of metastable domains-walls that perfectly explains the observed trends of the splitting of the 1/3 plateau at low temperatures, and verify that the latter has long-range order at the equilibrium. To be consistent with the previous existing models, we use the same set of parameters for the Hamiltonian [30, 31, 32], namely, an interchain antiferromagnetic interaction, $J = J_\mathrm{inter} = 2.25$ μeV, and a large Ising magnetic moment, $S = 32$. Disorder or dispersive effects in the exchange coupling constant were not required to obtain the splitting of the 1/3 plateau, as it will become clear in the following. Therefore, our model and methods are different from Yao *et al.* [31, 32], and we concentrate our efforts mainly to describe the effects of the sweeping rate on the observed metastable states, that generate the sub-steps in the magnetization.

II. MONTE-CARLO SIMULATIONS IN 2D

The spin-chain compound $Ca_3Co_2O_6$ is formed by close-packed one-dimensional chains along the c-axis, the chains span a triangular lattice over the ab-plane. Due to such geometric configuration and the hierarchy of the exchange interactions, the system can be modeled as a two-dimensional (2D) antiferromagnetic Ising model with nearest-neighbor exchange interactions [30, 31, 32]. The magnetic moments are representative of the $[Co_2O_6]_n$ chains, which are always perpendicular to the ab-plane. The choice of this frozen-moment model is a consequence of a time-scale assumption. We believe that the characteristic time involved in reversing the individual spins of each chain is much shorter than the rearrangement of the triangular lattice by changing the magnetic field. This hypothesis is based on previous numerical results [33] on nano-wires, as well as on the large number of sites that are involved in changing the whole triangular lattice as compared to those on a single spin-chain.

We thus performed Monte Carlo simulations using a triangular Ising model, where the magnetic moments are frozen, pointing either up or down, and coupled antiferromagnetically ($J > 0$) to their nearest neighbors. In this picture, the Hamiltonian $\mathcal{H}$ of the system is

$$\mathcal{H} = J \sum_{\langle i,j \rangle} S_i^z S_j^z - g\mu_\mathrm{B} \sum_i \mathbf{S}_i \cdot \mathbf{H}\,, \qquad (1)$$

where $\mathbf{S}_i$ is the spin of each magnetic moment, $\mathbf{H}$ is the external magnetic field along the $+c$-axis, $g = 2$ is the electronic Landé factor, μ_B the Bohr magneton and $\langle i,j \rangle$ indicates summation over all pairs of nearest-neighbors on a triangular lattice. We used a single-flip Monte Carlo method together with the standard Metropolis algorithm to reject/accept flips in the magnetization with a Boltzmann factor [34]. Magnetization measurement at any given field was done using 1,000 averages over a fixed number of *accepted* Monte-Carlo (MC) flips. We used different 2D finite cluster configurations, including super-hexagons, octagons, dodecagons and other more circularly-shaped geometries to represent the samples. The magnetization curves found in all these finite clusters were almost the same, the main difference was the number of MC flips needed to reach the plateaus for different sizes. Due to space limitations and visualization aspects, a selection of the results for one cluster size with hexagonal geometry was chosen. Extra material showing the evolution of magnetic configurations with the field can be found at the website by the interested reader [supplementary material].

III. MAGNETIZATION RESULTS

In this section we discuss our magnetization results by using Monte Carlo calculations on finite clusters with

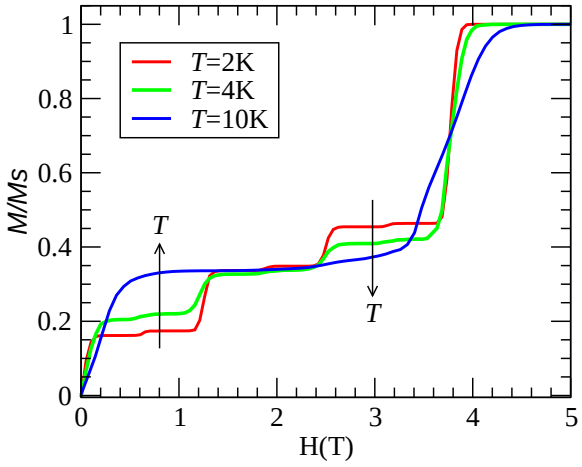

FIG. 2: MC results for the magnetization as a function of the applied field for three different temperatures in the ferrimagnetic phase, $T \leq 10$ K, and $N = 2431$ sites. The splitting of the 1/3 plateau into three successive plateaus is observed below 10 K. They extend up to fields $H \approx 1.2$ T, 2.4 T and 3.6 T, respectively. We see that they merge into a unique plateau at $M \approx M_s/3$ as T increases (see arrows).

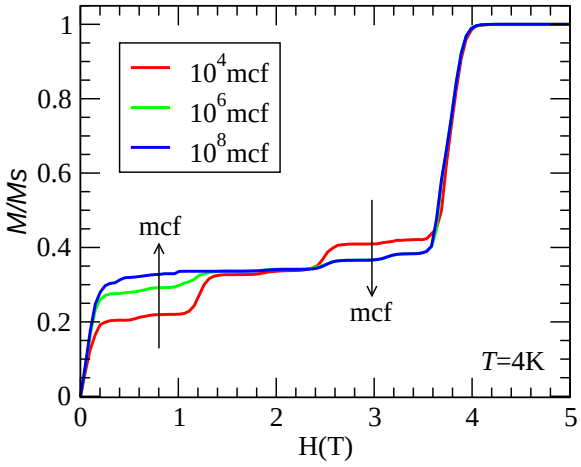

FIG. 3: MC results for the magnetization as a function of the applied field for three different sweep rates, at $T = 4$ K, and $N = 2431$ sites. This is accomplished by letting more or less accepted MC flips (mcf) per magnetic field. Notice the tendency of merging into the plateau $M_s/3$ as the number mcf increases (see arrows), indicating a time decay towards the 1/3 state. This behavior will be further analyzed.

open boundary conditions, always increasing the field, starting at $H = 0$ T. The initial magnetic state was obtained by thermalizing a random disordered configuration, performing 10^6 MC flips in a *training* period. Afterwards we initiated the increase of the field at a constant sweep rate. We calculated clusters with hexagonal geometries for $N = 1387$, 2431, 3169, 4921 and 6931 sites. Some other larger clusters were partially calculated, but we verified that the agreement with the experimental results did not improve with size. As the system size increased the plateaus structure remained unaltered, only small perturbations (sub-steps) on each of the three main plateaus tend to disappear.

In Figure 2 we readily observe the formation of three well defined plateaus below $T = 10$ K. Important to see is that they merge into one, at $M_s/3$ as T increases, indicating a close resemblance with the experimental situation (see e.g. Fig. 3 in [19]). The presence of extra tiny substeps is an unavoidable boundary effect due to the finiteness of the cluster used (in this case, $N = 2431$ sites). They are created by border isolated atoms whose contribution is strongly suppressed for larger cluster sizes, therefore, irrelevant for our argument. Another important feature to note in the results of Figure 2, shared by experiments, is the steeper rise of the magnetization for lower temperatures at the end of the 1/3 plateau ($H_c \approx 3.6$ T).

Now, as a way to check how stable are such plateaus, we have performed MC analyses with an increasing number of steps per magnetic field. In fact, as the MC simulation is done with the accepted configurations, what really counts is MC flips (mcf) and not MC steps (mcs). We clearly see, in Figure 3, the tendency to merge the three plateaus into one as a function of the number of mcf. This certainly must be related to the experimental sweeping rate [19]. This connexion allows us to say that the three plateaus are metastable states and are, therefore, a dynamical effect; for this very reason the experimental magnetization curves are strongly dependent on the sweeping rate [19].

This merging effect can be further explained in the graph of Figure 4, where we have produced an almost perfect superposition between magnetization curves for different temperatures and, at the same time, different mcf. In such a case, we tried to draw a parallel between the mcf in our simulation and the sweeping rate in the experimental results, where this behavior is observed. It is obvious from this result the strong interplay between the effects of time and temperature (see e.g. Fig. 4 in [19]), a feature that was previously used as a fingerprint of QTM. Although mcf are *not* related to lab time measurement, we can attribute them to some sweeping rate by comparing the formation of the plateaus. Hence, the three sub-plateaus are made of metastable states, which develop in time to the 1/3 plateau, as in Figure 3.

Dipolar interactions were also considered, as an intrinsic effect always present in nanowires and other low-dimensional systems, but its overall effect here was merely to induce an effective antiferromagnetic field that retarded the field at which the steps occur. The dipolar term $\mathcal{H}_{\rm dip}$ that was added to equation (1) is given by:

$$\mathcal{H}_{\rm dip} = \frac{1}{2}\sum_{i,j} \frac{\mathbf{m}_i\cdot\mathbf{m}_j - 3(\mathbf{m}_i\cdot\hat{\mathbf{r}}_{ij})(\mathbf{m}_j\cdot\hat{\mathbf{r}}_{ij})}{r_{ij}^3} \qquad (2)$$

where the summation is over all sites, and $\mathbf{m}_i = \pm\mu_{\rm B}\mathbf{S}_i$.

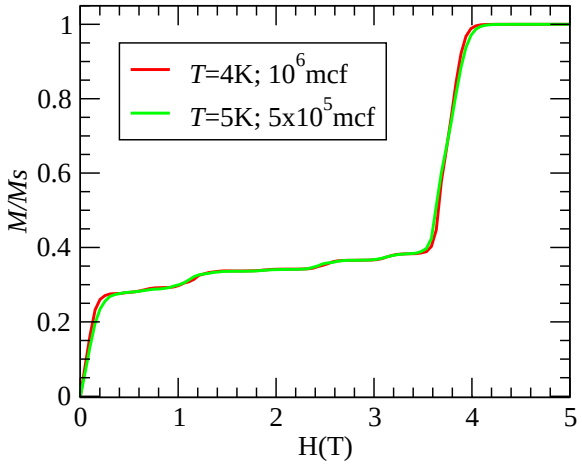

FIG. 4: Magnetization versus applied field for two different temperatures and different sweep rates. We see that they merge into very similar curves. This overlap indicates that they correspond to the same statistical configuration, one which realizes similar magnetic moments. Such *scaling* is an extra indication of metastable configurations. Differences are seen at both steep rising regions, close to zero and at $H_c \approx 3.6$ T, fact which is also seen in the experiments [19].

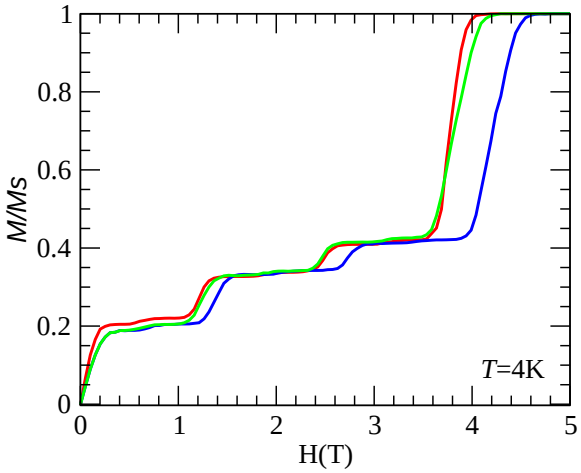

FIG. 5: Magnetization versus applied field considering dipolar interactions, at $T = 4$ K, and $N = 2431$ sites. The red curve is for the original J value used in Figure 3, without dipolar interaction. The blue curve is for the same J, but now with dipolar interaction, and the green curve is for a reduced exchange, 90% of the original value, and the same dipolar interaction of the blue curve. The scaling of the red and the green curves is not perfect, but very close.

We see such effect in Figure 5, with the dipolar interaction playing the role of an effective antiferromagnetic field, $H \to H + H_{\text{eff}}$ added to equation (1), that moves the magnetization curves to the right. We noticed that adjusting the exchange constant to $0.9J$, we can almost reproduce the results obtained from our previous 2D Ising model, without dipolar interaction (see Figure 5). For this reason, we think, the magnetization curves are well described using only the exchange and Zeeman terms.

IV. SNAPSHOTS AND DOMAIN-WALLS

The physics behind these results can be visualized by using raw snapshots of selected configurations. In the next pictures we show different snapshots of the magnetization curves depicted with the red line of Figure 3. They were taken at three different magnetic fields: $H = 0.81$ T, $H = 2.0$ T, and $H = 2.98$ T, representative of each of the three sub-steps, into which the 1/3 plateau is splitted at low temperatures ($T < 10$ K).

Our color convention to analyze the snapshots of the subsequent examples is depicted in Figure 6. Following [9], we define four triangles and color them differently depending on the magnetization that results by summing the three spins at their vertices: see Figure 6.

Configurations at zero field are formed by disordered bicontinuous patterns of small compact regions of violet and green phases, with total zero magnetization. For a field close to 0.25 T, domain walls, as seen in Figure 7, stabilize their motion to quasi-static domain walls until the field reach values of about 1.2 T.

Moving the field across the boundary, $H = 1.2$ T, produces a rapid rearrangement of the linked domain walls positions, by changing simultaneously their internal configuration. They are now formed by mixed violet and red triangles, as shown in Figure 8. They rate together to zero extra magnetic moment, sometimes oscilating above and below, depending slightly on the simulation parameters. The magnetic configuration in Figure 8 averages to zero, leading to $M = M_s/3$, the value of the green ordered zone (formed by the hexagonal unit cells).

Finally, for fields beyond the other boundary, $H = 2.4$ T, the situation is quite different. Now the linked domain walls are formed mostly by red colored triangles (Figure 9) with a tendency to coalesce in small groups, or seeds, at the borders of the simulated clusters. This interesting feature of red seeds at the boundaries, as seen

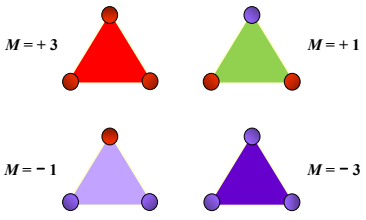

FIG. 6: The magnetic moment of each triangle depends on the orientation of each ferromagnetic chain. The four possibilities are schematized by different colors, but $M = -3$ is seldom seen for positive magnetic fields in the following snapshots.

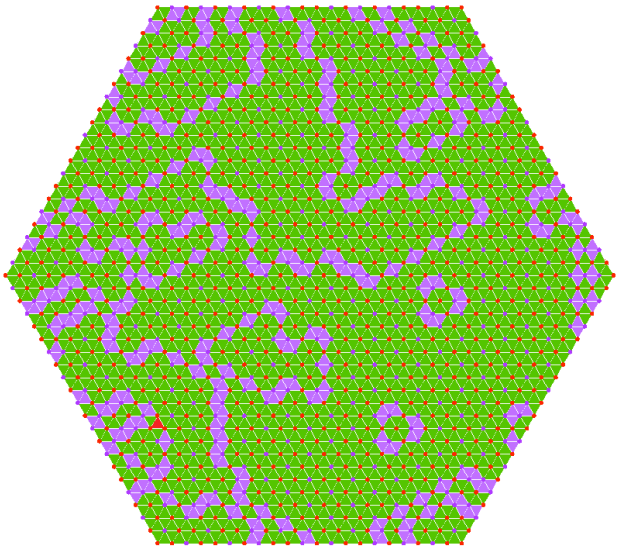

FIG. 7: Snapshot of a particular magnetic configuration in an hexagonal cluster of 1387 spins, at the first sub-step, of field $H = 0.81$ T, at $T = 4$ K and 10^4 mcf, as depicted with a red line in Figure 3. Notice the ordered substrate green zone, with $M = M_s/3$, superimposed by interlinked domain walls, formed mostly by connected triangles in violet color. These domain walls contribute to a reduction of the $M_s/3$ value of the green zone to $M \approx 0.22 M_s$, in this example.

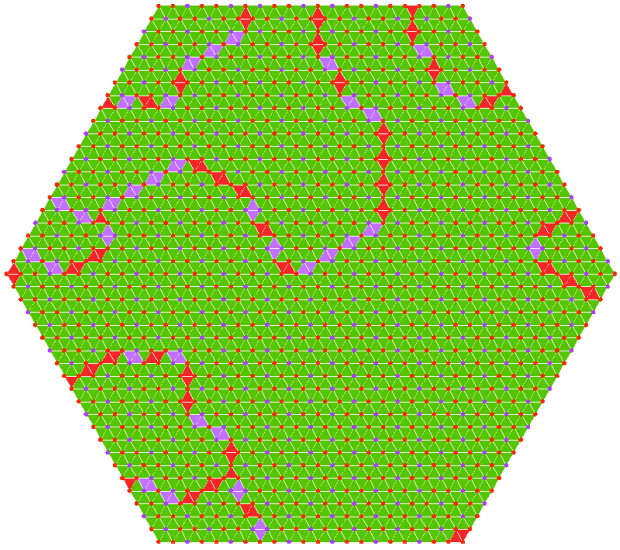

FIG. 8: Same parameters as in Figure 7, except at a higher field $H = 2.0$ T, corresponding to a magnetization value of $0.33 M_s$ in this case. Observe now the green extended zone superimposed by linked domain walls of mixed violet and red colored triangles, in a proportion that contribute almost zero extra moment. These linked domain walls, as those before, percolate throughout the system and are rather stable across a finite window of the magnetic field: 1.2 T $< H <$ 2.4 T.

in Figure 9, is a peculiar phenomena very similar to pre-nucleation phases, as found in irreversible statistical mechanics studies. Proper nucleation really starts beyond the critical field, $H_c = 3.6$ T, in this way: first coalescence of small red seeds at the borders and then myriads of red nuclei forming and growing, taking account of the whole cluster, in the bulk, until saturation. The nucleation process above H_c is a very rapid, disordered one, destroying the linked domain walls structures seen in the former examples. Perfect alignment is only achieved at the end, for fields higher than 4 T.

All these non-equilibrium phenomena just described were obtained for a particular sweep rate, of 10^4 mcf. We tested various sweep rates, observing similar behavior for many of them. But, none of these metastable interlinked domain walls were present, however, when we go beyond a sweep rate of 10^9 mcf. In that case, the disordered initial phase goes immediately to the 1/3 plateau, and beyond $H_c = 3.6$ T, to saturation. Such 1/3 plateau is represented solely by the green zone, without any further domain wall, thus of long-range nature. Therefore, we believe our characterization of such metastable states, sweep-rate dependent, must be related to the multi-step phases of $Ca_3Co_2O_6$, found experimentally at low T.

V. TRIANGULAR CLUSTERS

In this section, we show how the 1/3 plateau of the Ising model of previous sections shares interesting similarities with the simplest small clusters of triangular geometry. A generic spin Hamiltonian for these clusters is the following Heisenberg Hamiltonian:

$$\mathcal{H} = \frac{1}{2}\sum_{i,j}^{N} J_{ij}\mathbf{S}_i\cdot\mathbf{S}_j - \delta\sum_{i}^{N}(\mathbf{S}_i\cdot\hat{\mathbf{n}})^2 - g\mu_{\rm B}\sum_{i}^{N}\mathbf{S}_i\cdot\mathbf{H} \quad (3)$$

Results for a triangular molecule are shown in Figure 10. M (the thermal average of the total spin z-component) is zero only at zero field, and it increases rapidly to the 1/3 plateau for any finite H, crossing through $H = h_1$ until $H = h_2$, where it rapidly increases again to saturation. Such a transition is first-order at $T = 0$ only. Increasing the temperature produces a smooth growing up of M due to thermal fluctuations. Notice that larger thermal fluctuations accelerate this trend above h_1 and retard it above h_2, as seen from Figure 10.

Interesting to note is that such a trend in Figure 10 resembles the MC solution of the Ising model in the triangular lattice of our previous sections. Although it is not the same behavior, a tendency to form a 1/3 plateau is without any doubt. No further sub-plateaus can possibly be observed in a triangular molecule because of lack of phase space. Domain walls in the Ising dynamics are minimally formed by triangles, as seen before.

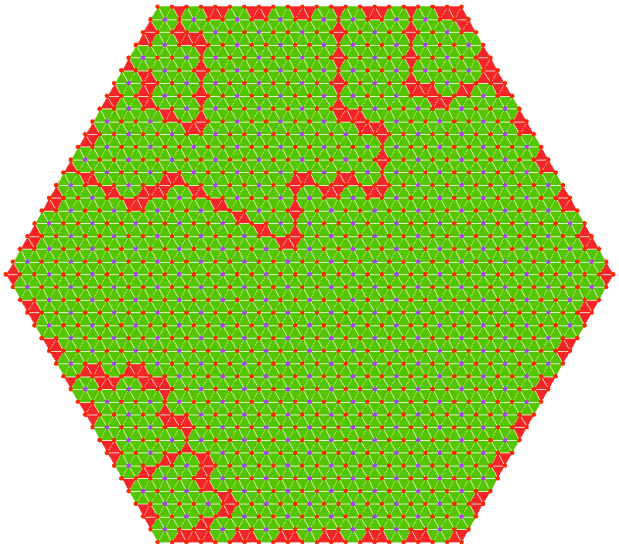

FIG. 9: Snapshot of the third sub-plateau, at a field $H = 2.98$ T. Other parameters as in Figures 7 and 8. The magnetic configuration is now formed by the green extended region of $M = M_s/3$ superimposed by domain walls in red color, giving a total magnetization of $0.41M_s$, in this case. Notice also some red seeds distributed at the borders of the cluster, like in pre-nucleation phases of irreversible studies. Nucleation really starts beyond the critical field, $H_c = 3.6$ T.

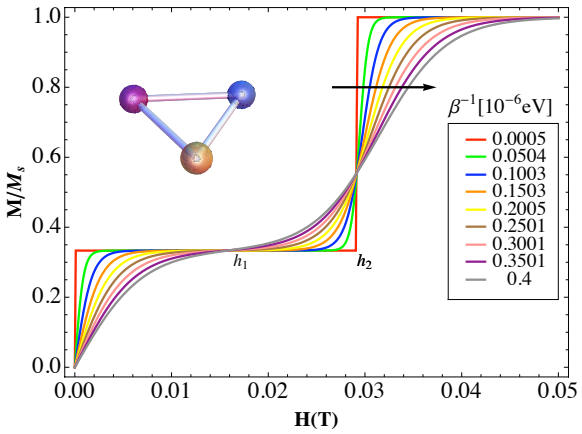

FIG. 10: Exact magnetization against a magnetic field for the Heisenberg triangular molecule ($N = 3$), and for different temperatures, $\beta^{-1} = k_B T$, as shown in the legend. We see a tendency to form a 1/3 plateau. Other parameters used are: $J = 2.25$ μeV, $\delta = 1$ μeV, and $S = 1/2$.

Further supporting arguments come from numerical exact solutions for (larger) finite clusters. In Figure 11 we see, for example, numerical results for the magnetization of the pure Heisenberg model in the triangular lattice, in the absence of anisotropy, at $T = 0$, for $N = 36$ and 39 sites [38]. The formation of a clear 1/3 plateau of finite width, ΔH, is seen from the graphic. Such results have

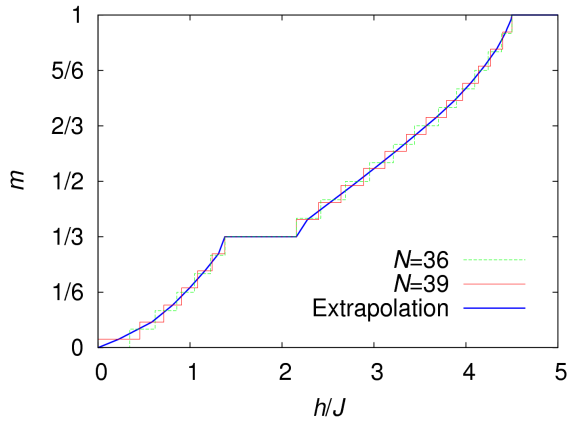

FIG. 11: Exact magnetization against a magnetic field for Heisenberg triangular clusters at $T = 0$, $\delta = 0$, and $S = 1/2$. The green and red lines are for $N = 36$ and 39 sites, while the bold blue line is an extrapolation to the thermodynamic limit (see text). Notice the 1/3 plateau of finite width ΔH [38].

been taken in the literature [39, 40, 41, 42] as the evidence of a definite plateau in the thermodynamic limit: the bold line in Figure 11 was drawn by connecting the midpoints of the finite-size steps for $N = 39$ sites, except at the boundaries of the 1/3 plateau. A good estimate for the lower and upper fields of the boundaries of the exact 1/3 plateau in the triangular lattice were obtained comparing spin-wave and exact diagonalization results. They are given by $H_\ell = 1.378J$ and $H_u = 2.155J$, respectively. See more recent results in [42].

To better understand our point, we should recall that both models, Ising and Heisenberg, show a similar behavior – with a 1/3 plateau – because the magnetic field already breaks the symmetry from $SU(2)$ to $U(1)$, thus making the strong quantum fluctuations inoperant in the isotropic Heisenberg triangular case and, consequently, the $M = 1/3$ state becomes a classical, collinear state, with long-range order.

VI. CONCLUSION AND FINAL REMARKS

In summary, we did an extensive investigation of the triangular lattice using Monte Carlo simulation techniques. We studied this lattice using a 2D Ising model for large magnetic moments coupled antiferromagnetically. We were motivated by multiple steps observed in the magnetization of the spin-chain $Ca_3Co_2O_6$ compound. We found a very good agreement between our results and the experimental situation [19]. We demonstrated that the observed plateaus of the ferrimagnetic phase, below $T \leq 10$ K, consist of metastable states and for this reason are time-dependent. In the experimental results such dependence was observed in the sweeping rate of the magnetic field, and in our case this dependence comes

from the number of Monte Carlo flips (mcf). In fact, a close parallelism is found between these two approaches, as seen from our Figures 2, 3, 4, and Figures 3, 4, 5 from Ref. [19]. Besides such agreement, we also found that in the limit of very large number of mcf, namely, a very slow rate of the field, the three sub-steps converge into one plateau, at $M/M_s = 1/3$, like in the experiments, thus giving a thermal decay of such metastable states into the equilibrium, final 1/3 plateau, which has long-range hexagonal order (described by the green ordered zone of the snapshots, with an hexagon as unit cell).

Further analysis using snapshots of some specific configurations revealed the presence of linked (mobile) domain-walls that give origin to the splitting of the 1/3 plateau below $T \leq 10$ K, as explained in the text. Such a result disproves the possibility of quantum tunneling as generating the multiple steps, at least for temperatures above 4 K, and for the reported sweep rates. Based on our results, we believe that at lower temperatures an arrested configuration may provide a slower dynamics of the domain-walls, that would explain a T-independent time-decay process below 4 K, by critical slowing down, an aspect that certainly must still be checked down.

Our solution has been checked by further considering the intrinsic dipolar interactions, finding no relevant contribution from such couplings. We therefore discarded them as possible contribution of hysteresis phenomena which are strongly present at the ferrimagnetic region, below 10 K, in the experiments [19]. We believe that other ingredients and methods, like 3D simulations, must be considered to deal with such irreversible aspects, but this is beyond our model of the magnetization plateaus.

Another point that we wanted to emphasize was linked to exact solutions of the Heisenberg model in the triangular lattice for finite clusters. We did a comparison with our previous numerical Ising solution and found supporting arguments with the presence of the 1/3 plateau in the isotropic Heisenberg case at $T = 0$. Both models share the 1/3 plateau, although for different reasons. In the quantum-mechanical case the applied magnetic field strengthens the frustration effects in the triangular lattice up to a point of having sufficient overlap with the classical, collinear, three-fold degenerate, 1/3 plateau [41]. The point here is that the presence of the 1/3 plateau in the isotropic quantum limit does not require a strong uniaxial anisotropy. Although we did not a thermal study of the exact solution of the Heisenberg model, a feature hard to be done, we think that at low temperatures the 1/3 plateau would survive to thermal fluctuations in order to be observed numerically. Such a comparison, therefore, strongly supports our thermal, classical study of the spin-chain compound, $Ca_3Co_2O_6$.

While this paper was considered for publication we became aware of another work, by Kudasov *et al.* [43], on the same problem, namely, a study of the dynamics of magnetization in frustrated spin-chain system $Ca_3Co_2O_6$ using a 2D model. Although they present similar results for the magnetization steps, they are complementary to ours in some respects.

Acknowledgments

This work was partially supported by Fondecyt grant number 1070224, CONICYT Ph.D. Fellowship Millennium Science Initiative under Project P06-022-F and also supported by CNPq (Brasil). One of us (GM) would like to acknowledge the Universidad Técnica Federico Santa María, in Valparaíso, Chile, for a sabbatical stay. We also thank Dr. Andreas Honecker for sharing his data on the triangular lattice.

[1] M. Oshikawa, M. Yamanaka, and I. Affleck, Phys. Rev. Lett. **78**, 1984 (1997).
[2] D. C. Cabra, A. Honecker, and P. Pujol, Phys. Rev. Lett. **79**, 5126 (1997).
[3] T. Vekua, D. C. Cabra, A. Dobry, C. Gazza, and D. Poilblanc, Phys. Rev. Lett. **96**, 117205 (2006).
[4] I. J. Hamad, L. O. Manuel, G. Martínez, and A. E. Trumper, Phys. Rev. B **74**, 094417 (2006).
[5] M. F. Collins and O. A. Petrenko, Can. J. Phys. **75**, 605 (1997).
[6] H. Fjellvåg, E. Gulbrandsen, S. Aasland, A. Olsen, and B. C. Hauback, J. Solid State Chem. **124**, 190 (1996).
[7] S. Aasland, H. Fjellvåg, and B. Hauback, Solid State Commun. **101**, 187 (1997).
[8] H. Kageyama, K. Yoshimura, K. Kosuge, H. Mitamura, and T. Goto, J. Phys. Soc. Jpn. **66**, 1607 (1997).
[9] A. Maignan, C. Michel, A. C. Masset, C. Martin, and B. Raveau, Eur. Phys. J. B **15**, 657 (2000).
[10] B. Martínez, V. Laukhin, M. Hernando, J. Fontcuberta, M. Parras, and J. M. González-Calbet, Phys. Rev. B **64**, 012417 (2001).
[11] B. Raquet, M. N. Baibich, J. M. Broto, H. Rakoto, S. Lambert, and A. Maignan, Phys. Rev. B **65**, 104442 (2002).
[12] V. Hardy, M. R. Lees, A. Maignan, S. Hébert, D. Flahaut, C. Martin, and D. M. Paul, J. Phys.: Condens. Matter **15**, 5737 (2003).
[13] R. Vidya, P. Ravindran, H. Fjellvåg, A. Kjekshus, and O. Eriksson, Phys. Rev. Lett. **91**, 186404 (2003).
[14] V. Hardy, S. Lambert, M. R. Lees, and D. McK. Paul, Phys. Rev. B **68**, 014424 (2003).
[15] M.-H. Whangbo, D. Dai, H.-J. Koo, and S. Jobic, Solid State Commun. **125**, 413 (2003).
[16] A. Maignan, V. Hardy, S. Hébert, M. Drillon, M. R. Lees, O. Petrenko, D. Mc K. Paul, and D. Khomskii, J. Mater. Chem. **14**, 1231 (2004).
[17] R. Frésard, C. Laschinger, T. Kopp, and V. Eyert, Phys. Rev. B **69**, 140405(R) (2004).
[18] V. Eyert, C. Laschinger, T. Kopp, and R. Frésard, Chem. Phys. Lett. **385**, 249 (2004).

[19] V. Hardy, M. R. Lees, O. A. Petrenko, D. McK. Paul, D. Flahaut, S. Hébert, and A. Maignan, Phys. Rev. B **70**, 064424 (2004).

[20] D. Flahaut, A. Maignan, S. Hebert, C. Martin, R. Retoux, and V. Hardy, Phys. Rev. B **70**, 094418 (2004).

[21] V. Hardy, D. Flahaut, M. R. Lees, and O. A. Petrenko, Phys. Rev. B **70**, 214439 (2004).

[22] A. Villesuzanne and M.-H. Whangbo, Inorg. Chem. **44**, 6339 (2005).

[23] K. Takubo, T. Mizokawa, S. Hirata, J.-Y. Son, A. Fujimori, D. Topwal, D. D. Sarma, S. Rayaprol, and E.-V. Sampathkumaran, Phys. Rev. B **71**, 073406 (2005).

[24] K. Yamada, Z. Honda, J. Luo, and H. Katori, J. Alloys Compd. **423**, 188 (2006).

[25] Hua Wu, M. W. Haverkort, Z. Hu, D. I. Khomskii, and L. H. Tjeng, Phys. Rev. Lett. **95**, 186401 (2005).

[26] Hua Wu, Z. Hu, D. I. Khomskii, and L. H. Tjeng, Phys. Rev. B **75**, 245118 (2007).

[27] W. Wernsdorfer, M. Murugesu, and G. Christou, Phys. Rev. Lett. **96**, 057208 (2006).

[28] M. R. Wegewijs, C. Romeike, H. Schoeller, and W. Hofstetter, New J. Phys. **9**, 344 (2007).

[29] For a review, see *Quantum Tunneling of Magnetization*, edited by L. Gunther and B. Barbara (Kluwer, Dordrecht, 1995).

[30] Yuri B. Kudasov, Phys. Rev. Lett. **76**, 027212 (2006).

[31] X. Y. Yao, S. Dong, and J.-M Liu, Phys. Rev. B **73**, 212415 (2006).

[32] X. Y. Yao, S. Dong, H. Yu, and J.-M Liu, Phys. Rev. B **74**, 134421 (2006).

[33] M. Vázquez, K. Nielsch, P. Vargas, J. Velázquez, D. Navas, K. Pirota, M. Hernández-Velez, E. Vogel, J. Cartes, R. B. Wehrspohn and U. Gosele, Physica B **343** 395 (2004); M. Vázquez, M. Hernández-Velez, K. Pirota, A. Asenjo, D. Navas, J. Velázquez, P. Vargas and C. Ramos, Eur. Phys. J. B **40**, 489 (2004).

[34] D. P. Landau and K. Binder, *A Guide to Monte Carlo Simulations in Statistical Physics*, 2nd. Edition (Cambridge University Press, 2005).

[35] K. Y. Choi, Y. H. Matsuda, H. Nojiri, U. Kortz, F. Hussain, A. C. Stowe, C. Ramsey, and N. S. Dalal, Phys. Rev. Lett. **96**, 107202 (2006).

[36] S. Carretta, P. Santini, G. Amoretti, F. Troiani, and M. Affronte, Phys. Rev. B **76**, 024408 (2007).

[37] K. Y. Choi, N. S. Dalal, A. P. Reyes, P. L. Kuhns, Y. H. Matsuda, H. Nojiri, S. S. Mal, and U. Kortz, Phys. Rev. B **77**, 024406 (2008).

[38] A. Honecker, *private communication.*

[39] B. Bernu, P. Lecheminant, C. Lhuillier, and L. Pierre, Phys. Rev. B **50**, 10048 (1994).

[40] A. Honecker, J. Phys.: Condens. Matter **11**, 4697 (1999).

[41] A. Honecker, J. Schulenburg, and J. Richter, J. Phys.: Condens. Matter **16**, S749 (2004).

[42] U. Schollwöck, J. Richter, D. J. J. Farnell, R. F. Bishop (Eds.), *Quantum Magnetism* (Springer, Berlin, 2004).

[43] Yu. B. Kudasov, A. S. Korshunov, V. N. Pavlov, and D. A. Maslov, Phys. Rev. B **78**, 132407 (2008).